



ARTICLE

Retro mode illumination for detecting and quantifying the area of geographic atrophy in non-neovascular age-related macular degeneration

Giulia Corradetti^{1,2,3}, Iksoo Byon^{1,4}, Federico Corvi^{1,5}, Mariano Cozzi⁵, Giovanni Staurenghi⁵ and Srinivas R. Sadda^{1,3}✉

© The Author(s), under exclusive licence to The Royal College of Ophthalmologists 2021

PURPOSE: To evaluate the ability of retro mode illumination imaging for quantifying atrophy compared to confocal color fundus photography (c-CFP), green light fundus autofluorescence (G-FAF), blue light fundus autofluorescence (B-FAF) using the scanning laser ophthalmoscope (SLO) Mirante device by Nidek (Nidek Co., Ltd, Gamogori, Japan).

METHODS: Eyes with clinical evidence of geographic atrophy (GA) associated with non-neovascular age-related macular degeneration, evaluated at the Doheny Eye Centers-UCLA and Hospital Sacco Milan, were included in this prospective, cross-sectional study. All eyes were imaged with multiple retinal imaging modalities using the SLO Nidek Mirante device: c-CFP, G-FAF, B-FAF, retro mode illumination deviated-right (RMDR), and deviated-left (RMDL). Masked graders measured the GA lesion on each modality and inter-modality and inter-grader repeatability were assessed.

RESULTS: The mean (SD) area of GA measured 9.76 (3.82) mm², 9.75 (3.91) mm², 9.76 (3.92) mm², 9.82 (3.87) mm², and 9.81 (3.86) mm² using c-CFP, G-FAF, B-FAF, RMDR, and RMDL, respectively ($p = 0.2$). Inter-modality correlation was high (Pearson's $r > 0.9$ and $p < 0.0001$). Agreement between graders was excellent for all modalities.

CONCLUSIONS: Retro mode imaging demonstrated good agreement for measuring GA compared to other imaging modalities, with a high level of repeatability. Given that retro mode imaging uses infrared light and is comfortable, it may prove to be a useful tool for the assessment of GA in the clinic.

Eye (2022) 36:1560–1566; <https://doi.org/10.1038/s41433-021-01670-3>

INTRODUCTION

Age-related macular degeneration (AMD) is a leading cause of vision loss and blindness worldwide in developed nations [1]. Geographic atrophy (GA) is considered to be the late stage of the non-neovascular form of the disease [2]. GA is characterized by a well-demarcated area of loss of the retinal pigment epithelium (RPE), overlying photoreceptors, and underlying choriocapillaris (CC) and is most commonly monitored using flash color fundus photography (f-CFP) or fundus autofluorescence (FAF) [3–5]. Quantification of GA by FAF has been introduced as a primary outcome parameter in clinical trials for non-neovascular AMD for regulatory approval [3, 6–9]. The major contributor to the autofluorescence from the posterior segment of the eye is lipofuscin, a material that accumulates within RPE cells. Thus, lipofuscin can provide insight into the integrity of RPE, and the loss of the lipofuscin signal can suggest loss or dysfunction of the RPE or their overlying photoreceptors [10]. Compared with f-CFP where the borders of the GA lesion may be difficult to identify in some cases in the absence of good stereopsis, the high contrast of FAF imaging allows the GA lesion to be delineated reliably. FAF imaging, however, is not without disadvantages. One of the

limitations, particularly when blue-light FAF is used, is that the central macular luteal pigment absorbs blue light resulting in hypofluorescence centrally which may make a determination of foveal involvement by the GA lesion difficult [11]. Another disadvantage of FAF is the intense short-wavelength light may be uncomfortable for patients and there are theoretical concerns for retinal toxicity with blue light exposure [12–17]. GA lesions are also well-seen on optical coherence tomography (OCT), which has the additional advantage that the specific layers involved by the atrophic process can be directly visualized. Recently, the Classification of AMD Meetings (CAM) group proposed a consensus definition for atrophy on OCT, termed complete RPE and outer retinal atrophy (cRORA) based on a constellation features: (1) a region of hyper transmission of ≥ 250 μm in diameter, (2) a zone of continuous attenuation or disruption of the RPE of ≥ 250 μm in diameter, (3) evidence of overlying photoreceptor degeneration, and (4) absence of scrolled RPE or other signs of an RPE tear [18]. Although the CAM proposed that OCT could be used as the base or reference modality to identify atrophy, they recommended that a multimodal imaging approach may provide the most complete assessment of the atrophic lesion [3]. The

¹Doheny Eye Institute, Los Angeles, CA, USA. ²Retina Disorders and Ophthalmic Genetics, Stein Eye Institute, University of California-Los Angeles, Los Angeles, CA, USA. ³Department of Ophthalmology, David Geffen School of Medicine at UCLA, Los Angeles, CA, USA. ⁴Department of Ophthalmology, Research Institute for Convergence of Biomedical Science and Technology, Pusan National University Yangsan Hospital, Pusan National University School of Medicine, Yangsan, South Korea. ⁵Eye Clinic, Department of Biomedical and Clinical Science “Luigi Sacco”, Sacco Hospital, University of Milan, Milan, Italy. ✉email: SSadda@doheny.org

Received: 28 December 2020 Revised: 11 June 2021 Accepted: 23 June 2021

Published online: 14 July 2021

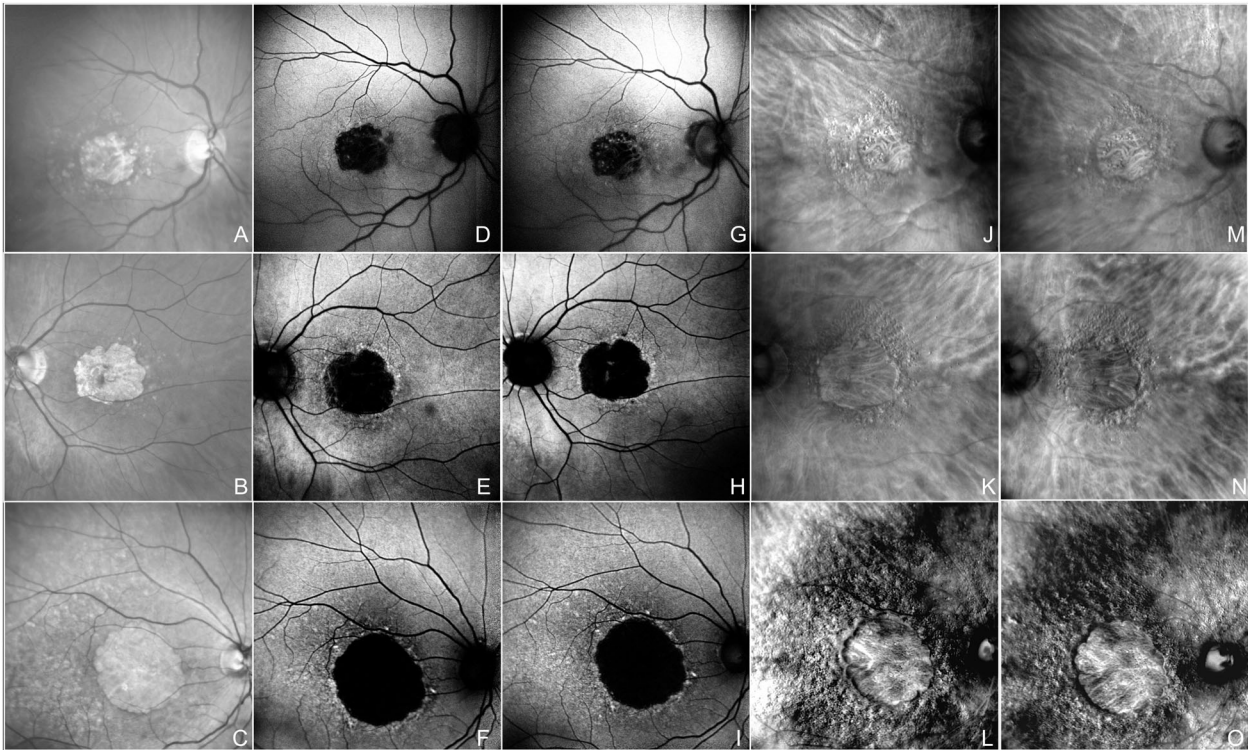


Fig. 1 Composite of multimodal imaging in three subjects (one for each line) with late-stage age-related macular degeneration and evidence of geographic atrophy included in this study. All SLO modalities clearly show geographic atrophy involving the foveal center. The confocal SLO true color (red, green, and blue lasers) fundus photographs (A, B, C) highlights the central area of geographic atrophy as a region of depigmentation with increased visibility of the choroidal vessels. The fundus region involved by the atrophic changes is outlined by well-demarcated borders, which are sometimes more difficult to discern with standard flash photographs. Blue-light (D, E, F) and green-light autofluorescence (G, H, I) nicely show the central hypoautofluorescent patch with high contrast due to loss of RPE cells associated with GA. For each subject, retro mode illumination images were acquired using the deviated-right (J, K, L) and deviated-left mode (M, N, O). In retro mode illumination, the geographic atrophy lesions are represented by pseudo-three-dimensional circular patches with homogenous reflectivity and evident underlying hyperreflective choroidal vessels. [GA geographic atrophy, SLO scanning laser ophthalmoscopy, RPE retinal pigment epithelium].

information from the various imaging modalities may be complementary. For example, the FAF patterns surrounding the GA lesion may predict the rate of progression or enlargement of the atrophy. In this study, we evaluate a newer imaging modality, retro mode illumination imaging, which provides greater contrast for identifying fundus lesions at different depths. In this analysis, we specifically compare the ability and reliability of retro mode illumination for quantifying atrophy compared to c-CFP, B-FAF, and G-FAF.

METHODS

This is a prospective, observational, cross-sectional, multicentre study. The study adhered to the tenets of the Declaration of Helsinki and Health Insurance Portability and Accountability Act and was approved by the UCLA Institutional Review Board (IRB Ocular Imaging Study) and by the Luigi Sacco Hospital Ethics Committee in Milan.

Subjects enrollment

Consecutive patients over the age of 55 with a clinical diagnosis of non-neovascular late-stage AMD [19] with evidence of subfoveal geographic atrophy in one or both eyes who were evaluated between March 2019 and January 2020 at the retina clinics of the Doheny UCLA - Eye Center and the Luigi Sacco Hospital - Milan were considered eligible for this study. Geographic atrophy was recognized as a well-demarcated area of depigmentation associated with visible underlying choroidal vessels on fundus ophthalmoscopy and confirmed by the presence of cRORA [18] (OCT Spectralis Heidelberg; Germany) as defined in CAM Report 3. Eyes with any history of anti-vascular endothelial growth factors (VEGF) injections or evidence of macular atrophy associated with macular

neovascularization were excluded. We also excluded eyes with clinically significant media opacity or any other evidence of retinal disease. Written informed consent was obtained from all subjects prior to enrollment. All patients underwent a complete ophthalmological examination, including best-correct visual acuity (BCVA), slit-lamp biomicroscopy, and dilated ophthalmoscopy. BCVA was expressed using the logarithmic scale of the minimum angle of resolution (logMAR), but was measured using the Snellen chart.

Imaging

All eyes included in the study were imaged using the SLO Mirante device (Mirante, Nidek Co., Ltd, Gamagori, Japan) with five different modalities: confocal color fundus photography (c-CFP), green light fundus autofluorescence (G-FAF), blue light fundus autofluorescence (B-FAF), retro mode illumination deviated right (RMDR) and retro mode illumination deviated left (RMDL). (Fig. 1)

Confocal SLO Mirante color fundus images are obtained using three different laser wavelengths (red, 670 nm; blue, 488 nm; green, 532 nm) coupled to a specific dedicated sensor for each wavelength. The resultant true color SLO fundus image is acquired at a resolution of 1536×1536 pixels (averaged 3x).

Green-light fundus autofluorescence and blue-light fundus autofluorescence are generated using excitation wavelengths of 488 nm and 532 nm, respectively, at a resolution of 1024×1024 pixels (averaged 60x). Retro mode illumination is a relatively novel imaging modality in which the typical central confocal aperture of an SLO device is substituted by a laterally deviated circular aperture, which may be deviated-right (DR) or deviated-left (DL). The scattered light going through the lateral (right or left) aperture generates a shadow, enhancing the contrast for deeper structures such as the RPE, producing a pseudo-three-dimensional image [20–23]. Retro mode illumination uses near-infrared wavelength (790 nm)

light to generate a monochromatic image and is acquired at a resolution of 1536×1536 pixels (averaged 50x). On retro mode illumination, GA lesions manifest as well-demarcated regions, which appear depressed as a result of the pseudo-three-dimensional contrast and also show evidence of choroidal vessels (hypo-reflective signal) within the bed of atrophy (Fig. 2). All images from all modalities were acquired with the same field of view of 89° . Images with poor quality or demonstrating atrophy which extended beyond the borders of the image were not included in the final analysis.

Grading protocol

Images were exported from the SLO Mirante device and imported into Image J for quantitative analysis. Experienced, independent, and masked retina specialist graders (GC, IB) independently delineated the borders of the area of geographic atrophy using Image J. Different modalities from the same eye were analysed and annotated on different days to minimize "recall bias" from one imaging modality when grading another imaging modality of the same eye. For each GA lesion, outlined the total area expressed in mm^2 was automatically computed using ImageJ.

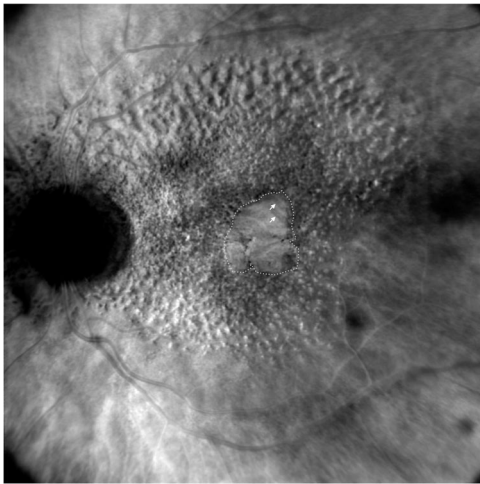


Fig. 2 Case of geographic atrophy and drusen associated with age-related macular degeneration in a 89-year old subject imaged using retro mode deviated-right illumination imaging by SLO Nidek Mirante device. The retro mode illumination imaging produces a monochromatic image. The geographic atrophy lesion (within the green dotted line) is clearly highlighted and characterized by pseudo-three dimensional lesion with homogenous reflectivity and well-defined borders. The atrophic changes allow the visualization of the underlying choroidal vessels (white arrow). [SLO scanning laser ophthalmoscopy].

Statistical analysis

The statistical analyses were performed using SPSS software v.26.0 (IBM Corp, Armonk, New York, USA). Descriptive statistics were used to assess the frequencies for categorical variables and compute the mean (SD) for continuous variables. The Shapiro–Wilk test was used to assess the normality of sample distribution for the continuous variables. One-way ANOVA analysis for repeated measures was computed to determine the inter-modality variability in the measurements of GA areas (mm^2). Bland–Altman plots were used to illustrate the limits of agreement among all ten possible pairwise comparisons in the measurements of the area of GA for the different modalities. Likewise, Pearson's r analysis was calculated to assess the correlation among all different imaging modalities to determine whether measurement variability was dependent on the imaging modality. For each imaging modality (c-CFP, G-FAF, B-FAF, RMDR, RMDL), the absolute inter-grader difference, the coefficient of variation (CV), and the two-way random absolute agreement intraclass correlation coefficient (ICC) were calculated. In addition, differences in the measurements of the area of GA between the two graders were plotted using Bland–Altman graphs. Statistical significance was set at a p value <0.05 .

RESULTS

Forty eyes of forty subjects (27 female, 67.5%) with AMD and clinical evidence of GA were enrolled in the study. Mean \pm SD age of the enrolled subjects was 78.07 ± 7.4 (range 65–91 years). Mean BCVA \pm SD measured 0.59 ± 0.18 logMAR (Snellen range 20/40–20/100). Twenty-seven eyes showed a unifocal pattern of GA as defined by FAF (67.5%). Table 1 shows demographics data and clinical features of the eyes included in the analysis.

Table 1. Demographics and clinical data of subjects included in the analysis.

Demographics and clinical data	
Subjects enrolled, n	40
OD, n (%)	25 (62.5)
Age, mean (SD); range	78.07 (7.4); 65–91
Gender, F (%)	27 (67.5)
BCVA logMAR, mean (SD)	0.59 (0.18)
BCVA Snellen range	20/40–20/100
Pattern of GA lesions; n (%)	Multifocal 13 (32.5) Unifocal 27 (67.5)

n Number, OD Right eye, SD Standard deviation, F female, BCVA Best Corrected Visual Acuity, GA Geographic atrophy.

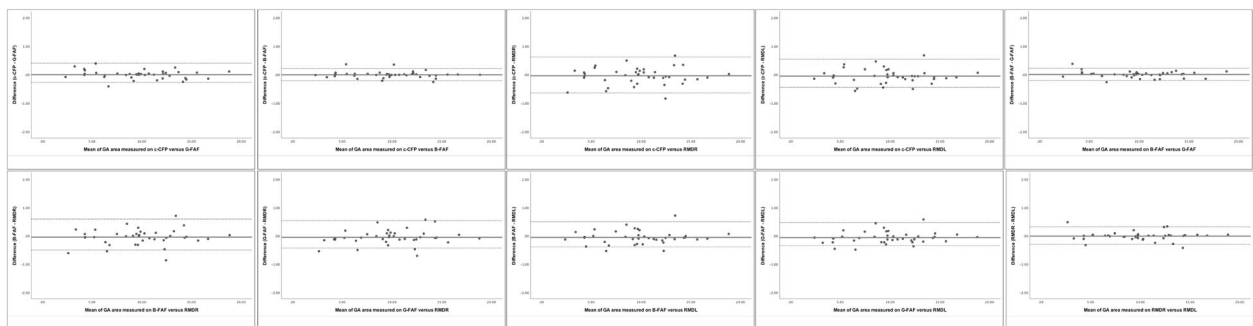


Fig. 3 Bland–Altman plots assessing the inter-modalities agreement in the measurements of the area of geographic atrophy measured on SLO Mirante device using five different modalities. The composite illustrates the ten possible pairwise inter-modalities comparisons. The red line indicates the mean difference between the different modalities, the green dashed line indicates the upper and lower limit of agreement and the black dashed line indicates the zero difference in the measurements of the GA area using different modalities available on the SLO Mirante device. [c-CFP confocal color fundus photography, GA geographic atrophy, G-FAF green-light fundus autofluorescence, B-FAF blue-light autofluorescence, RMDR retro mode deviated-right, RMDL retro mode deviated-left, SLO Scanning Laser Ophthalmoscopy].

Inter-modality GA area measurements

The mean (SD) area of GA measured 9.76 (3.89) mm², 9.75 (3.91) mm², 9.76 (3.92) mm², 9.82 (3.87) mm², 9.81 (3.86) mm² using c-CFP, G-FAF, B-FAF, RMDR and RMDL, respectively. A one-way repeated measures ANOVA was conducted to determine whether there was a statistically significant difference in the GA area measurements among the five different imaging modalities. The data were normally distributed for each modality, as assessed by Shapiro–Wilk test ($p > 0.05$). No statistically significant differences were detected among the five different imaging modalities in the measurements of GA area, $F(4, 1.471) = 1.47$, $p = 0.2$ according to the one-way repeated measures ANOVA. Figure 3 shows the agreement between modalities plotted using the Bland–Altman analysis of the ten possible pairwise comparisons and demonstrates a high level of consistency. Furthermore, the Pearson's r analysis revealed a high correlation between mean GA area measurements among the different imaging modalities with $r > 0.90$ ($p < 0.0001$) for all ten possible pairwise comparisons.

Inter-grader agreement

The mean absolute inter-reader difference in GA area measurements was 0.06 ($p = 0.47$) for c-CFP, 0.05 ($p = 0.54$) for G-FAF, 0.06 ($p = 0.52$) for B-FAF, 0.06 ($p = 0.59$) for RMDR, and 0.1 ($p = 0.41$) for RMDL. The mean intraclass correlation coefficient (ICC) for absolute measurements was 0.98 (95% CI 0.97–0.99; $p < 0.0001$) for c-CFP, 0.99 (95% CI 0.98–0.99; $p < 0.0001$) for G-FAF, 0.98 (95% CI 0.97–0.99; $p < 0.0001$) for B-FAF, 0.98 (95% CI 0.96–0.99; $p < 0.0001$) for RMDR and 0.98 (95% CI 0.96–0.99; $p < 0.005$) for RMDL. Similarly, the CV demonstrated a high degree of consistency in GA area measurements across all modalities (0.04 for c-CFP, 0.03 for G-FAF, 0.04 for B-FAF, 0.05 for RMDR, and 0.05 for RMDL). The inter-grader agreement results are shown in Table 2. For each modality, Bland–Altman plots were used to illustrate the trend in GA area measurement differences between graders (Fig. 4).

DISCUSSION

In this study, we compared five different SLO retinal imaging modalities for their ability to quantify the area of GA in eyes with non-neovascular AMD and observed no statistically significant difference between modalities (one-way repeated measures ANOVA: $F(4, 1.471) = 1.47$, $p = 0.2$). Furthermore, the mean difference in measured area between modalities ranged between 0.05 and 0.1 mm² and they were highly correlated ($r > 0.9$ and $p < 0.0001$). In addition, all modalities demonstrated a very high level of agreement between graders for measuring GA lesion area (Table 2, Fig. 4). In most ongoing clinical trials, the quantification of GA area has been performed using a confocal SLO blue-light FAF (excitation wavelength of 488 nm, emission bandwidth of 500–700 nm) [24–26]. The death of RPE and photoreceptors in GA is associated with loss of lipofuscin and consequently appears on blue-light FAF as an area with extinguished autofluorescence [26, 27]. The high contrast between the atrophic and the perilesional retinal tissue allows a highly precise and accurate measurement of the GA area. With advances in retinal imaging, researchers have investigated the use of various imaging modalities for the measurement of GA lesions in eyes with AMD.

In 2012, Khanifar et al. [28] compared measurements of GA areas on both f-CFP and FAF images and described a high intra-observer agreement between f-CFP and FAF, suggesting that both imaging modalities provide similar measurements of GA area. In fact, in most cases, the difference in measurements between the two modalities was close to zero, with a higher coefficient of variation for f-CFP [28]. The inter-grader repeatability was also high. Domalpally et al. quantified the area of GA lesions using color photographs and corresponding fundus autofluorescence, using a larger cohort (Age-related Eye Disease Study 2–AREDS2 ancillary study) and found that the GA area measurements in

Table 2. Comparison of measurements of GA atrophy from five imaging modalities using SLO Nidek Mirante device and inter-grader agreement.

	c-CFP	G-FAF	B-FAF	RMDR	RMDL
GA area (mm ²), mean (SD), range	9.76 (3.89); 2.31–8.84	9.75 (3.91); 2.32–18.73	9.76 (3.92); 2.31–18.85	9.82 (3.87); 2.92–18.82	9.81 (3.86); 2.44–18.78
Absolute inter-reader difference (p value)	0.06 (0.47)	0.05 (0.54)	0.06 (0.52)	0.06 (0.59)	0.1 (0.41)
CV	0.04	0.03	0.04	0.05	0.05
ICC (95% CI); p value	0.98 (0.97–0.99); $p < 0.0001$	0.99 (0.98–0.99); $p < 0.0001$	0.98 (0.97–0.99); $p < 0.0001$	0.98 (0.96–0.99); $p < 0.0001$	0.98 (0.96–0.99); $p < 0.0001$

c-CFP Confocal color fundus photography, G-FAF Green-light fundus autofluorescence, B-FAF Blue-light fundus autofluorescence, RMDR Retro mode illumination deviated-right, RMDL Retro mode illumination deviated-left, GA Geographic atrophy, SD Standard deviation, CV Coefficient of variation, ICC Intraclass correlation coefficient.

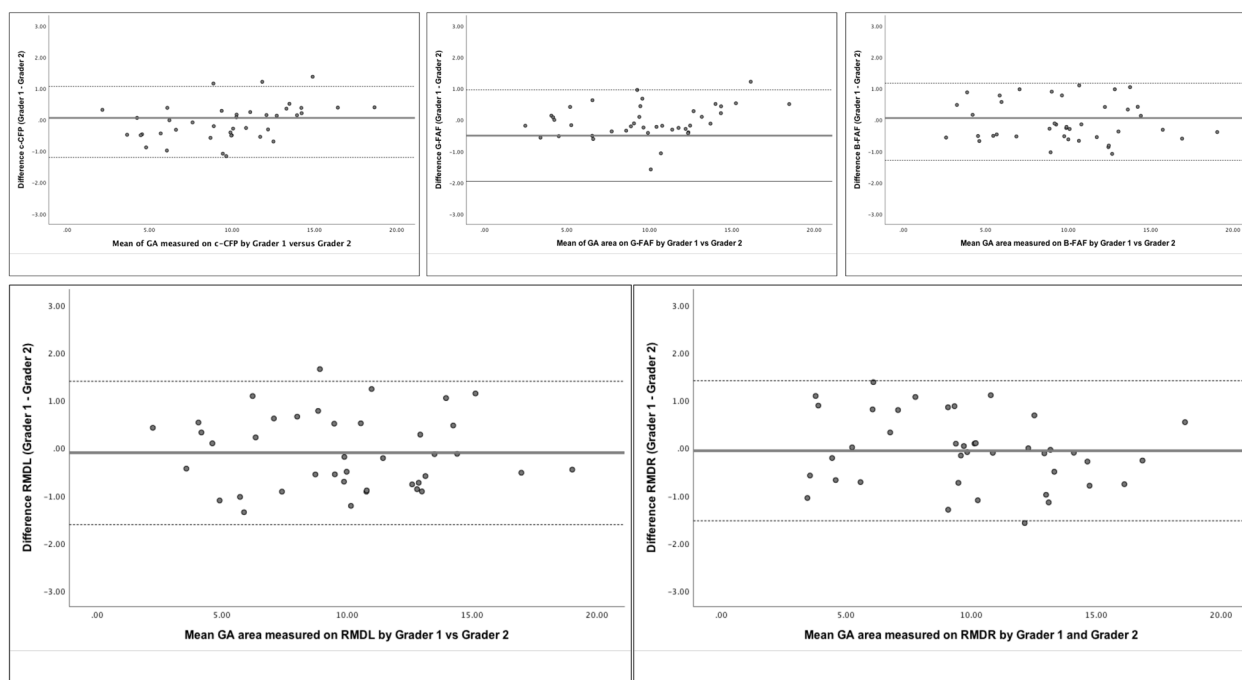


Fig. 4 Bland-Altman plots showing the inter-graders agreement in the measurement of GA atrophy using the five different modalities on SLO Nidek Mirante device. Grader 1 and Grader 2 showed a high degree of concordance in outlining the area of GA in eyes with non-neovascular age-related macular degeneration using c-CFP, G-FAF, B-FAF, RMDR and RMDL. [GA geographic atrophy, SLO Scanning Laser Ophthalmoscopy, c-CFP confocal color fundus photography, G-FAF green-light fundus autofluorescence, B-FAF blue-light fundus autofluorescence, RMDR retro mode illumination deviated-right, RMDL retro mode illumination deviated-left].

fundus stereoscopic color photography and fundus autofluorescence were similar across all visits (mean difference 0.5 mm^2) [29]. In our study, we observed a similar finding with no statistically significant difference in GA measurements across the various imaging modalities (one-way repeated measures ANOVA: $F(4, 1.471) = 1.47, p = 0.2$). In contrast, the GAP study (Geographic Atrophy Progression Study) reported significant differences in the measurements of GA areas between CFP and B-FAF although the measurements were highly correlated [7]. However, in the GAP study, the FAF annotations were performed by a semi-automated algorithm, whereas in our analysis all GA lesions were manually segmented. Wong et al. [30] described excellent agreement between GA areas, as quantified by standard CFP and FAF (Spearman correlation, $r = 0.986$), although slightly yet statistically significant larger areas were measured on FAF. Several groups have also evaluated the potential of en face spectral-domain optical coherence tomography (SD-OCT) for assessment of GA area [31–34]. Yehoshua et al. observed no statistically significant difference in average GA area measurements when comparing en face SD-OCT images to FAF images [31]. SD-OCT offers the additional advantage of cross-sectional B-scans images which allows the layers impacted by the atrophy to study precisely. More recently, Cleland et al. demonstrated that GA area measurements using SD-OCT B-scans, based on the CAM cRORA criteria, are reproducible [35]. They also noted that when GA is measured on en face OCT based on the presence of choroidal hypertransmission, the lesion measured larger than c-CFP, infrared, or FAF, though the differences were not statistically significant. To our knowledge, ours is the first study to evaluate retro mode imaging for the assessment of atrophy in AMD. In retro mode imaging, the scattered light is blocked centrally and passes through a lateral aperture (deviated-right or deviated-left), which creates a shadow that effectively yields a pseudo-three-dimensional image [20–22]. In our study, the area of GA measured by retro mode was numerically larger compared to other modalities, though the differences were small and not statistically significant.

Furthermore, the inter-grader reproducibility for GA measurements by retro mode was very high, and numerically similar compared to all other modalities. It should be noted that the inter-grader reproducibility for all modalities in this study was high, which may be a reflection of the fact that poor-quality images were excluded from the analysis. Recently, Cozzi et al. [23] investigated the capability of retro mode imaging for the detection of drusen and suggested that this technology may be able to detect subtle drusen with higher sensitivity and specificity compared to other retinal imaging modalities. In the present study, the area of GA measured by retro mode was similar to other modalities (no statistically significant difference), but was numerically larger. It is possible that retro mode imaging may be more sensitive for the detection of subtle atrophic changes that are not apparent on FAF or CFP. However, this will require further evaluation in larger studies that are powered to detect small differences, as well as the use of pixel-overlap analyses to specifically evaluate discrepant regions. Retro mode illumination offers some important advantages over other imaging modalities for GA. Patients do not experience the discomfort that is commonly reported from the intense flash associated with CFP or the blue/green-light FAF imaging. Also, unlike blue-light FAF (the current clinical trials gold standard for GA assessment), retro mode is not impacted by the presence of luteal pigment which can confound the assessment of the fovea. In addition, the longer wavelength (790 nm) allows better penetration and potentially better quality in situations of media opacity. Although it was not specifically evaluated in this study, retro mode may be superior to conventional infrared reflectance (IR) imaging, as the pseudo-3-D effect makes the borders of depressed lesions easier to identify. However, this hypothesis needs to be evaluated in a future study. One limitation of retro mode imaging is that in eyes with significant media opacity or poor fixation, the quality of the image may not be uniform across the entire field of view, and shadow artifacts may be observed in the periphery. As the GA lesions are often centrally positioned, this is usually not problematic in most

cases, but maybe an issue in eyes with very large lesions. Our study has several limitations that should be taken into consideration when evaluating our findings. First, the sample size was relatively small and the majority of lesions were unifocal. Thus, we cannot extrapolate our observations to specific lesion phenotypes that were not evaluated in large numbers in our analysis. However, this is a pilot study to assess the feasibility for retro mode in this application, and the high level of inter-grader reliability is a promising finding. Second, we only included eyes with atrophy associated with non-neovascular AMD, excluding all other forms of macular atrophy. Third, we did not compare OCT measurements of atrophy in this analysis, primarily because dense OCT B-scan volumes were not obtained. This can be a topic of future analysis. Our study also has strengths, including the use of experienced, masked, and independent graders, a standardized grading protocol, and a prospective design. In summary, retro mode imaging showed good agreement with other planar imaging modalities for assessment of GA area, and a high level of reproducibility. As retro mode imaging has some potential advantages over these other modalities, its feasibility for use in clinical practice and clinical trials of GA warrants further evaluation.

Summary

What was known before

- In most ongoing clinical trials, the quantification of GA area has been performed using a confocal SLO blue-light FAF. The death of RPE and photoreceptors in GA is associated with loss of lipofuscin and consequently appears on blue-light FAF as an area with extinguished autofluorescence. The high contrast between the atrophic and the perilesional retinal tissue allows a highly precise and accurate measurement of the GA area.

What this study adds

- To our knowledge, ours is the first study to evaluate retro mode imaging for the assessment of atrophy in AMD. Retro mode imaging showed good agreement with other planar imaging modalities for assessment of GA area, and a high level of reproducibility.

REFERENCES

1. Wong WL, Su X, Li X, Cheung CM, Klein R, Wong TY. Global prevalence of age-related macular degeneration and disease burden projection for 2020 and 2040: a systematic review and meta-analysis. *Lancet Glob health*. 2014;2:e106–e116.
2. Fleckenstein M, Mitchell P, Freund KB, Sadda SR, Holz FG, Brittain C, et al. The progression of geographic atrophy secondary to age-related macular degeneration. *Ophthalmology*. 2018;125:369–90.
3. Holz FG, Sadda SR, Staurengi G, Lindner M, Bird AC, Blodi BA, et al. Imaging protocols in clinical studies in advanced age-related macular degeneration: recommendations from classification of atrophy consensus meetings. *Ophthalmology*. 2017;124:464–78.
4. Schmitz-Valckenberg S, Sadda S, Staurengi G, Chew EY, Fleckenstein M, Holz FG, et al. Geographic atrophy: semantic considerations and literature review. *Retina*. 2016;36:2250–64.
5. Gass JD. *Stereoscopic atlas of macular diseases*, Ed 1.; Oxford: Blackwell; 1970.
6. Holz FG, Strauss EC, Schmitz-Valckenberg S, van Lookeren Campagne M. Geographic atrophy: clinical features and potential therapeutic approaches. *Ophthalmology*. 2014;121:1079–91.
7. Schmitz-Valckenberg S, Sahel JA, Danis R, Fleckenstein M, Jaffe GJ, Wolf S, et al. Natural history of geographic atrophy progression secondary to age-related macular degeneration (geographic atrophy progression study). *Ophthalmology*. 2016;123:361–8.
8. Csaky K, Ferris F, Chew EY, Nair P, Cheetham JK, Duncan JL. Report from the NEI/FDA endpoints workshop on age-related macular degeneration and inherited retinal diseases. *Investigative Ophthalmol Vis Sci*. 2017;58:3456–63.
9. Sadda SR, Chakravarthy U, Birch DG, Staurengi G, Henry EC, Brittain C. Clinical endpoints for the study of geographic atrophy secondary to age-related macular degeneration. *Retina*. 2016;36:1806–22.
10. Schmitz-Valckenberg S, Fleckenstein M, Scholl HPN, Holz FG. Fundus autofluorescence and progression of age-related macular degeneration. *Surv Ophthalmol*. 2009;54:96–117.
11. Schmitz-Valckenberg S, Fleckenstein M, Helb HM, Charbel Issa P, Scholl HP, Holz FG. In vivo imaging of foveal sparing in geographic atrophy secondary to age-related macular degeneration. *Investigative Ophthalmol Vis Sci*. 2009;50:3915–21.
12. Sparrow JR, Gregory-Roberts E, Yamamoto K, Blonska A, Ghosh SK, Ueda K, et al. The bisretinoids of retinal pigment epithelium. *Prog Retinal Eye Res*. 2012;31:121–35.
13. Borrelli E, Nittala MG, Abdelfattah NS, Lei J, Hariri AH, Shi Y, et al. Comparison of short-wavelength blue-light autofluorescence and conventional blue-light autofluorescence in geographic atrophy. *Br J Ophthalmol*. 2018;103:610–6.
14. Hammer M, Richter S, Kobuch K, Mata N, Schweitzer D. Intrinsic tissue fluorescence in an organotypic perfusion culture of the porcine ocular fundus exposed to blue light and free radicals. *Graefes Arch Clin Exp Ophthalmol*. 2008;246:979–88.
15. Youssef PN, Sheibani N, Albert DM. Retinal light toxicity. *Eye*. 2011;25:1–14.
16. Arnault E, Barrau C, Nanteau C, Gondouin P, Bigot K, Vienot F, et al. Phototoxic action spectrum on a retinal pigment epithelium model of age-related macular degeneration exposed to sunlight normalized conditions. *PLoS ONE*. 2013;8:e71398.
17. Wolffe M. How safe is the light during ophthalmic diagnosis and surgery. *Eye (Basingstoke)*. 2016;30:186–8.
18. Sadda SR, Guymer R, Holz FG, Schmitz-Valckenberg S, Curcio CA, Bird AC, et al. Consensus definition for atrophy associated with age-related macular degeneration on OCT. *Ophthalmology*. 2018;125:537–48.
19. Ferris FL, Wilkinson CP, Bird A, Chakravarthy U, Chew E, Csaky K, et al. Clinical classification of age-related macular degeneration. *Ophthalmology*. 2013;120:844–51.
20. Acton JH, Cubbidge RP, King H, Galsworthy P, Gibson JM. Drusen detection in retro-mode imaging by a scanning laser ophthalmoscope. *Acta Ophthalmologica*. 2011;89:E404–11.
21. Ohkoshi K, Tsuike E, Kitaoka T, Yamaguchi T. Visualization of subthreshold micropulse diode laser photocoagulation by scanning laser ophthalmoscopy in the retro mode. *Am J Ophthalmol*. 2010;150:856–62.
22. Diniz B, Ribeiro RM, Rodger DC, Maia M, Sadda S. Drusen detection by confocal aperture-modulated infrared scanning laser ophthalmoscopy. *Br J Ophthalmol*. 2013;97:285–90.
23. Cozzi M, Monteduro D, Parrulli S, Corvi F, Zicarelli F, Corradetti G, et al. Sensitivity and specificity of multimodal imaging in characterizing drusen. *Ophthalmol Retin*. 2020;4:987–95.
24. Schmitz-Valckenberg S, Bindewald-Wittich A, Dolar-Szczasny J, Dolar-Szczasny J, Dreyhaupt J, Wolf S, et al. Correlation between the area of increased autofluorescence surrounding geographic atrophy and disease progression in patients with AMD. *Investigative Ophthalmol Vis Sci*. 2006;47:2648–54.
25. Holz FG, Bindewald-Wittich A, Fleckenstein M, Dreyhaupt J, Scholl HPN, Schmitz-Valckenberg S. Progression of geographic atrophy and impact of fundus autofluorescence patterns in age-related macular degeneration. *Am J Ophthalmol*. 2007;143:463–72. e2.
26. Schmitz-Valckenberg S, Jorzik J, Unnebrink K, Holz FG. Analysis of digital scanning laser ophthalmoscopy fundus autofluorescence images of geographic atrophy in advanced age-related macular degeneration. *Graefes Arch Clin Exp Ophthalmol*. 2002;240:73–8.
27. Von Rückmann A, Schmidt KG, Fitzke FW, Bird AC, Jacobi KW. Fundus autofluorescence in patients with macular dystrophies, malattia leventinese, dominant drusen and age-related drusen. *Klinische Monatsblätter fur Augenheilkd*. 1998;213:81–6.
28. Khanifar AA, Lederer DE, Ghodasra JH, Stinnett SS, Lee JJ, Cousins SW, et al. Comparison of color fundus photographs and fundus autofluorescence images in measuring geographic atrophy area. *Retina*. 2012;32:1884–91.
29. Domalpally A, Danis R, Agrón E, Blodi B, Clemons T, Chew E. Evaluation of geographic atrophy from color photographs and fundus autofluorescence images: age-related eye disease study 2 report number 11. *Ophthalmology*. 2016;123:2401–7.
30. Wong WT, Kam W, Cunningham D, Harrington M, Hammel K, Meyerle CB, et al. Treatment of geographic atrophy by the topical administration of OT-551: results of a phase II clinical trial. *Investigative Ophthalmol Vis Sci*. 2010;51:6131–9.
31. Yehoshua Z, De Amorim Garcia Filho CA, Nunes RP, Gregori G, Penha FM, Moshfeghi AA, et al. Comparison of geographic atrophy growth rates using

- different imaging modalities in the COMPLETE study. *Ophthalmic Surg Lasers Imaging Retin.* 2015;46:413–22.
32. Fleckenstein M, Schmitz-Valckenberg S, Adrion C, Kramer I, Eter N, Helb HM, et al. Tracking progression with spectral-domain optical coherence tomography in geographic atrophy caused by age-related macular degeneration. *Investigative Ophthalmol Vis Sci.* 2010;51:3846–52.
 33. Bearelyly S, Chau FY, Koreishi A, Stinnett SS, Izatt JA, Toth CA. Spectral domain optical coherence tomography imaging of geographic atrophy margins. *Ophthalmology.* 2009;116:1762–9.
 34. Yehoshua Z, Garcia Filho CA, Penha FM, Gregori G, Stetson PF, Feuer WJ, et al. Comparison of geographic atrophy measurements from the OCT fundus image and the sub-RPE slab image. *Ophthalmic Surg Lasers Imaging Retin.* 2013;44:127–32.
 35. Cleland SC, Konda SM, Danis RP, Huang Y, Myers DJ, Blodi BA, et al. Quantification of geographic atrophy using spectral domain optical coherence tomography in age-related macular degeneration. *Ophthalmol Retin.* 2021;5:41–8.

ACKNOWLEDGEMENTS

The authors thank Keith Effert (Nidek Co. Ltd., Gamagori, Japan) for technical support.

AUTHOR CONTRIBUTIONS

GC: study conception, design, data acquisition, analysis, interpretation of data, drafting and revising, final approval. IB and FC: design, analysis, interpretation of data,

final approval. MC: data acquisition, revising, and final approval. GS: drafting and revising, final approval. SRS: study conception, design, interpretation of data, drafting and revising, final approval.

COMPETING INTERESTS

Giulia Corradetti: none; Iksoo Byon: none; Federico Corvi: none; Mariano Cozzi: Bayer (R), Nidek (R); Staurenghi Giovanni: Heidelberg Engineering (C), Optos (F), Ocular Instruments (P), OptoVue (F), CenterVue (C), Allergan (C), Bayer (C), Genentech (C), Novartis (C), Quantel Medical (C), Carl Zeiss Meditec (C), Appellis (C), Boheringer (C), Topcon (F), Roche (C). SriniVas Sadda: Amgen (C), Allergan (C), Genentech-Roche (C), Oxurion (C), Novartis (C), Regeneron (C), Bayer (C), 4DMT (C), Centervue (C, S), Heidelberg (C, F, S), Optos (C, F, S), Carl Zeiss Meditec (F, S), Nidek (S), Topcon (S).

ADDITIONAL INFORMATION

Correspondence and requests for materials should be addressed to S.R.S.

Reprints and permission information is available at <http://www.nature.com/reprints>

Publisher's note Springer Nature remains neutral with regard to jurisdictional claims in published maps and institutional affiliations.